DNA-BASED DELIVERY OF ANTI-DR5 NANOBODIES IMPROVES EXPOSURE AND ANTI-TUMOR EFFICACY OVER PROTEIN-BASED ADMINISTRATION

Giles Vermeire[1], Elien De Smidt[1,2], Peter Casteels[3], Nick Geukens[2], Paul Declerck[1,2], Kevin Hollevoet[1,2]

[1] Laboratory for Therapeutic and Diagnostic Antibodies, KU Leuven – University of Leuven, 3000 Leuven, Belgium

[2] PharmAbs, the KU Leuven Antibody Center – University of Leuven, 3000 Leuven, Belgium

[3] Nanobody Explorative Technologies, Ablynx - Technologiepark 21, 9052 Gent, Belgium

Correspondence should be addressed to Paul Declerck (paul.declerck@kuleuven.be) or Kevin Hollevoet (kevin.hollevoet@kuleuven.be). Address: Laboratory for Therapeutic and Diagnostic Antibodies, KU Leuven – Campus Gasthuisberg, O&N II Herestraat 49 box 820, 3000 Leuven, Belgium. Phone: +3216323431. Fax: +3216323460.

SHORT TITLE

DNA-based Nanobodies improve exposure and efficacy

ABSTRACT

Nanobodies present an appealing class of potential cancer therapeutics. The current study explores the *in vivo* expression of Nanobodies through DNA-encoded delivery. We hypothesized this approach could address the rapid clearance of Nanobodies and, through half-life modulation, increase the produced levels in circulation. We therefore evaluated pharmacokinetics and efficacy of variants of an anti-death receptor 5 Nanobody (NbDR5), either monovalent or multivalent with half-life extension properties, after DNA-based administration. Intramuscular electrotransfer of a monovalent NbDR5-encoding plasmid (pNbDR5) did not result in detectable plasma levels in BALB/c mice. A tetravalent NbDR5-encoding plasmid (pNbDR5$_4$) provided peak concentrations of 54 ng/mL, which remained above 24 ng/mL during a 12-week follow-up. DNA-based delivery of these Nanobody formats fused to a Nanobody binding to serum albumin (NbSA), pNbDR5-NbSA and pNbDR5$_4$-NbSA, resulted in significantly higher plasma levels, with peak titers of 5.2 µg/mL and 7.7 µg/mL, respectively. In an athymic nude mice COLO 205 colon cancer model, a quadrupled intramuscular DNA dose led to peak plasma levels of 270 ng/mL for pNbDR5$_4$ and 38 µg/mL for pNbDR5$_4$-NbSA. Potent anti-tumor responses were only observed for pNbDR5$_4$, following either intramuscular or intratumoral delivery. Despite comparable *in vitro* activity and superior plasma exposure, NbDR5$_4$-NbSA was less effective than NbDR5$_4$ *in vivo*, regardless of whether delivered as DNA or protein. Overall, DNA-based Nanobody delivery resulted in more potent and durable anti-tumor responses than protein-based Nanobody delivery. In conclusion, this study demonstrates pre-clinical proof of concept for DNA-based Nanobodies in oncology and highlights the improved outcome over conventional administration.

INTRODUCTION

Nanobodies® are 15-kDa immunoglobulin single variable domains that can be derived from camelids' heavy-chain-only antibodies, retaining full antigen-binding capacity (Nanobody® and Nanobodies® are registered trademarks of Ablynx NV) [1]. Due to their small size they have improved tissue penetration properties and can easily be engineered into multivalent formats capable of binding multiple targets. These features make them excellent drug candidates in the oncology space [2]. Nevertheless, their reduced dimension and lack of an Fc region results in faster clearance from circulation due to renal excretion [3]. Combining Nanobodies with DNA-based gene transfer could be a good strategy to address the inherent limitations of Nanobodies for therapeutic use.

DNA-based gene transfer of antibody-based therapeutics seeks to administer to patients the encoding plasmid DNA (pDNA), rather than the protein itself [4]. The subsequent prolonged *in vivo* expression presents a possible cost-efficient and time-saving alternative to the conventional production and administration. To assure effective uptake in the tissue, pDNA injection is typically combined with electroporation, both in a pre- and clinical context [5]. Our group previously demonstrated proof of concept for intramuscular DNA-based monoclonal antibody (mAb) gene transfer in mice and sheep, attaining µg/mL mAb levels for several months after pDNA electrotransfer [6,7,8]. Others have reported comparable mAb titers, typically ranging from single- to low double-digit µg/mL [9]. At the start of 2019, a first-in-human trial for intramuscular DNA-based mAb gene electrotransfer was initiated (ClinicalTrials.gov: NCT03831503), a landmark for the field. Despite the progress in the last decade, DNA-based gene transfer is still lagging behind compared to other platforms in terms of expression levels, which is especially relevant for antibody-based therapeutics [4].

The possible match between Nanobodies and DNA-based gene transfer is two-fold. First, we hypothesized that prolonged *in vivo* production could address the rapid clearance of

Nanobodies, overcoming the need for frequent and costly dosing regimens. DNA-based gene transfer thereby could present an addition to more classical half-life extension strategies, like PEGylation [10], increasing the valency of the Nanobody [11], and fusion to a serum albumin (SA)-binding Nanobody [3]. Second, we postulated that the *in vivo* expression of Nanobodies with an extended half-life could increase the titers in the bloodstream. Indeed, half-life extended Nanobodies remain longer in circulation, and the continuous production after gene transfer is expected to lead to higher accumulation.

In the present study, Nanobodies targeting death receptor 5 (DR5) served as a model, as their pre-clinical efficacy is well-characterized [12]. DR5, a receptor for tumor necrosis factor-related apoptosis-inducing ligand (TRAIL), is overexpressed in several cancer types and significantly correlated with poor survival [13]. Specific agonists of DR5, including TRAIL, mAbs and Nanobodies, have been developed to induce apoptosis of cancer cells. However, efficacy in clinical settings has been disappointing due to lack of response or due to on-target off-tumor toxicity [14,15].

This study aims to deliver pre-clinical proof of concept for DNA-based Nanobodies as a novel strategy in oncology. To investigate the compatibility of Nanobodies and DNA-based gene transfer, we evaluated the pharmacokinetics and efficacy of plasmid-encoded anti-DR5 Nanobodies in mice. The impact of multivalency and/or bispecificity on the pharmacokinetics was assessed by comparing intramuscular delivery of plasmids encoding for monovalent (pNbDR5) and tetravalent anti-DR5 Nanobodies ($pNbDR5_4$), as well as their respective anti-SA Nanobody fusion formats (pNbDR5-NbSA and $pNbDR5_4$-NbSA). Furthermore, efficacy of both intramuscular and intratumoral delivery of $pNbDR5_4$ and $pNbDR5_4$-NbSA was investigated in COLO 205, a well-characterized human colon-cancer-derived tumor model. Intramuscular DNA-based Nanobody gene transfer was thereby compared head-to-head with intravenous (IV) Nanobody protein administration.

MATERIALS AND METHODS

Design and production of Nanobody-encoding plasmids

All DNA-based anti-DR5 Nanobody formats (Figure 1) were designed using humanized monovalent anti-DR5 [16] and anti-SA [17] Nanobody sequences provided by Ablynx (Belgium). To build multimeric formats, monovalent Nanobody-encoding sequences were separated by seven repeats of a $Glycine_4$-Serine linker and preceded by a signal peptide from the mouse Ig heavy chain V precursor region. Constructs were codon-optimized for murine expression, synthesized by GeneWiz and subsequently cloned into a CAG-driven expression cassette in a previously described plasmid [7]. Cloning was verified via restriction analyses and *in vitro* expression. pDNA was produced in *E. coli* TOP10 strain and purified using the NucleoBond Xtra Maxi EF kit (Machery - Nagel) following the manufacturer's instructions. Purity was assessed via UV spectrophotometry, and integrity via agarose gel electrophoresis and sequencing (LGC Genomics). DNA was formulated and stored in D-PBS (no magnesium, no calcium, 14190144, Thermo Fischer Scientific).

Cell lines and reagents

293F Freestyle suspension cells (purchased from Thermo Fischer Scientific in 2015) were maintained in FreeStyle 293 expression medium (Thermo Fischer Scientific). CHO-S suspension cells (purchased from Thermo Fischer Scientific in 2018) were maintained in Freestyle CHO expression medium supplemented with 8 mM L-glutamine (Thermo Fischer Scientific). Cells were cultured in T175 flasks (Sarstedt, Germany) on an orbital shaker (Thermo Fischer Scientific) at 150 rpm and 8% CO_2 in a 37°C humidified incubator. The human colon cancer COLO 205 cell line (purchased from ATCC in 2018, CRL-1772) was maintained in RPMI medium 1640 supplemented with 10% heat-inactivated fetal bovine serum (Thermo Fischer Scientific). Cells were cultured in a 37°C humidified incubator at 5%

115 CO_2. Identity of the 293F cell line was confirmed in 2017 using short tandem repeat analysis
116 at the Laboratory of Forensic Biomedical Sciences, KU Leuven. For the CHO-S and COLO
117 205 cell line, an early-passage vial from the expanded master cell stock was used for all
118 experiments.
119
120 ***Mice***
121 Experiments were performed in five-week-old female athymic nude mice or eight-week-old
122 female BALB/c mice with an approximate weight of 18-22 grams. BALB/c (BALB/cAnNCrl)
123 mice were bred at the KU Leuven Animal Research Center. Athymic nude mice (hsd:
124 athymic-nude-foxn1<nu> nu/nu) were purchased at Envigo (The Netherlands). In the
125 pharmacokinetic experiments, 5 mice per group were used. In the efficacy studies, sample
126 sizes were 10 mice for intramuscular delivery and 8 mice for intratumoral delivery. These
127 numbers were based on our previous *in vivo* tumor studies [7,8]. Blood was collected through
128 retro-orbital bleeding, processed to plasma, and stored at -20°C until analysis. All animal
129 experiments were approved by the KU Leuven Animals Ethical Committee (project
130 P157/2017).
131
132 ***Human tumor xenograft mouse model***
133 Athymic nude mice were subcutaneously injected in the flank with 3 x 10^6 COLO 205 cells in
134 100 µl D-PBS. Tumor volume was measured three times per week and calculated using the
135 formula: $a \times b^2 \times 0.5$, with a being the tumor length and b the width. Measurements were done
136 in duplicate using a digital caliper (5OLD). Treatment was initiated once tumors became
137 palpable at a volume of 50-100 mm^3, typically five or six days post-injection. On the day of
138 the treatment, mice were randomized into treatment and control groups with equal distribution
139 of average tumor volume and weight. The investigator was not blinded to the group allocation

and outcome assessment. Mice were euthanized when tumors exceeded 2000 mm^3. No mice were excluded from the analyses.

pDNA electrotransfer in mice

Intramuscular pDNA electroporation was performed either in the right *tibialis anterior* muscle (BALB/c mice) or both *tibialis anterior* and *gastrocnemius* muscles (athymic nude mice). Intratumoral pDNA electroporation was performed directly in established subcutaneous tumors in athymic nude mice. Both intramuscular and intratumoral electroporation were done using previously optimized and validated pre-clinical protocols [7,8]. For intramuscular gene transfer in BALB/c mice, the skin was prepared using depilatory product (Veet, Reckitt Benckiser), at least one day prior to pDNA injection. Intramuscular delivery sites were injected with 40 µl of 0.4 U/µl hyaluronidase from bovine testes (H4272, Sigma, reconstituted in sterile saline), approximately one hour prior to pDNA electrotransfer. Intramuscular or intratumoral injections of 30 µl of pDNA, formulated in sterile D-PBS at 2 µg/µL for the largest construct or equimolar amounts for the other variants, were immediately followed by *in situ* electroporation using the NEPA21 Electroporator (Sonidel) with CUY650P5 tweezer electrodes at a fixed width of 5 mm. Signa Electrode Gel (Parker Laboratories) or Ultrasound Gel (Fiab) was applied to the muscle or tumor tissue, respectively, to decrease impedance below 0.4 Ohm. For intramuscular gene transfer in BALB/c mice, three series of four 20 ms square-wave pulses of 120 V/cm with a 50 ms interval were applied with polarity switching after two of the four pulses. The pulse field strength was increased to 160 V/cm to compensate for the higher impedance when electroporating athymic nude mice muscle. For intratumoral gene transfer, two series of four 5 ms square-wave pulses of 600 V/cm in perpendicular directions at a frequency of 1 Hz were applied. Pulse delivery was verified using the NEPA21 readout.

In vitro Nanobody production and purification

Mono- and bivalent Nanobodies (Figure 1, upper two formats) were produced *in vitro* in 293F cells and tetra- and pentavalent Nanobodies (Figure 1, lower two formats) in CHO-S cells. pDNA transfection and purification of the produced Nanobodies was done as described for mAbs [7]. Purified proteins were dialyzed twice to 20 mM sodium phosphate, 150 mM NaCl pH 7.5 or D-PBS, aliquoted and stored at -80°C. Purified Nanobodies were evaluated for antigen binding on an in-house designed indirect ELISA. Briefly, 96-well plates were coated overnight at 4°C with 250 ng/mL of TRAIL receptor 2 (DR5, 10465-H08H, Sino Biologicals). Blocking was performed using Superblock-PBS (Thermo Fischer Scientific) at room temperature for two hours. Nanobodies were diluted in PBS 0.1% BSA, 0.002% Tween 80 (PTA) and incubated at room temperature for one hour. Captured Nanobodies were detected using a rabbit polyclonal anti-Nanobody antibody (Ablynx, Belgium) and a goat anti-rabbit IgG-HRP antibody (GAR/IgG/PO, Novo Nordic). Both were incubated at room temperature for 1 hour (1:5 000 in PTA). Each incubation step was preceded by a washing step with PBS 0.05% Tween 20. O-phenylenediamine dihydrochloride substrate was applied for 15-30 minutes, followed by 4M H_2SO_4 to stop the reaction. Optical density (OD) was measured at 492 nm with an ELx808 ELISA reader (BioTek). Nanobody curves were plotted using Graphpad Prism 8.0 (Graphpad Software). Size and integrity of the Nanobodies was evaluated on SDS-PAGE (under non-reducing and dithiothreitol reducing conditions), respectively. For the latter, 500 ng of Nanobody was run on an Amersham PhastSystem SDS-PAGE according to the manufacturer's instructions.

Nanobody ELISAs

To quantify the Nanobodies in mouse plasma, multiple in-house sandwich-type ELISAs were designed. Briefly, 96-well plates were coated overnight at 4°C with 2 µg/mL of an anti-SA Nanobody binding mAb or an anti-DR5 Nanobody binding mAb (Ablynx, Belgium). Blocking was performed using Superblock-PBS at room temperature for two hours. Plasma samples were diluted in PBS 0.1% BSA, 0.002% Tween 80 with 5 mM EDTA (PTAE) and incubated at room temperature for one hour. Captured Nanobodies were detected using biotin-conjugated mouse anti-Nanobody mAbs (1:4000 dilution in PTA) and streptavidin-poly-HRP (Sanquin, 1:20000 dilution in PTA), incubated at room temperature and at 21°C, for one hour and 30 minutes, respectively. For detection, anti-Nanobody binding mAbs were biotinylated using EZ-Link Sulfo-NHS-LC-Biotin (#21335, Thermo Fischer Scientific), following the manufacturer's protocol. Substrate addition, plate readout and washing steps were performed identical to the above described ELISA. Nanobody concentrations were calculated using Graphpad Prism 8.0, based on a calibration curve obtained with the corresponding *in vitro* produced and purified Nanobody.

In vitro Nanobody activity

The *in vitro* biological activity of purified Nanobodies was evaluated in a WST-8 COLO 205 cell viability assay (Cell Counting Kit, Dojindo). Briefly, 10000 COLO 205 cells were seeded per well in 190 µL RPMI 1640 medium + 10% FBS in a 96-well plate and incubated in a 37°C humidified incubator at 5% CO_2. The following day, cells were incubated with Nanobody at different concentrations with our without varying concentrations of murine serum albumin (LifeSpan BioSciences). 48 hours following Nanobody administration, WST-8 was added and incubated at 37°C up to four hours, after which ODs were measured at 500 nm with an ELx808 ELISA reader (BioTek). All values were normalized to untreated cell controls (100 % viability) and no-cell wells with medium (0 % viability).

214

215 ***Statistics***

216 Statistical analyses and figure drawing were done using GraphPad Prism 8.0. Data were
217 presented as mean + standard error of the mean (SEM) and analyzed using ANOVA and
218 Tukey's multiple comparison test. Kaplan–Meier survival curves were analyzed with the
219 Gehan-Breslow-Wilcoxon test. P values were adjusted with a Holm's test for multiple
220 comparisons. Two-sided P values below 0.05 were considered significant.

RESULTS

In vitro expression and validation of Nanobody-encoding plasmids

The design of the Nanobody-encoding plasmids was based on two validated Nanobodies, one binding to human DR5 (anti-DR5 Nanobody, NbDR5), and one binding to human/mouse serum albumin (anti-SA Nanobody, NbSA). A panel of four Nanobody-encoding plasmids was generated, either expressing monovalent anti-DR5 Nanobody (pNbDR5, 4898 base pairs), tetravalent anti-DR5 Nanobody (pNbDR5$_4$, 6347 base pairs), bivalent bispecific anti-DR5-anti-SA Nanobody (pNbDR5-NbSA, 5372 base pairs) or pentavalent bispecific anti-DR5-anti-SA Nanobody (pNbDR5$_4$-NbSA, 6821 base pairs) (Figure 1). The monovalent anti-DR5 Nanobody is known not to exhibit any efficacy [12]. The DNA-based version thereof and the corresponding bispecific anti-SA Nanobody-fusion construct, were therefore included only for the pharmacokinetic evaluations (Figure 1).

All plasmids were first evaluated for their ability to express the corresponding functional Nanobody in 293F or CHO-S cell lines. *In vitro* produced Nanobody proteins showed the expected profile on SDS-PAGE (Figure S1A) and demonstrated binding to recombinant DR5 on ELISA (Figure S1B). Tetravalent anti-DR5 Nanobody (NbDR5$_4$) and pentavalent bispecific anti-DR5-anti-SA Nanobody (NbDR5$_4$-NbSA) demonstrated equivalent *in vitro* activity in a viability assay with COLO 205 cells, which are highly sensitive to TRAIL□ mediated cell death (Figure S1C) [18]. Together, these *in vitro* data indicate we generated functional Nanobody-encoding plasmids.

Pharmacokinetics of intramuscular DNA-based Nanobody gene transfer in BALB/c mice

We subsequently evaluated the *in vivo* pharmacokinetics of the expressed Nanobodies after intramuscular electrotransfer of the respective Nanobody-encoding pDNA in BALB/c mice. Equimolar doses were administered for pNbDR5 (55 µg, $n = 5$) and pNbDR5-NbSA (60 µg, n

= 5), as well as equimolar doses for pNbDR5$_4$ (55 µg, *n* = 5) and pNbDR5$_4$-NbSA (60 µg, *n* = 5).

Intramuscular gene transfer led to detectable plasma levels for all variants except for the monovalent anti-DR5 Nanobody (NbDR5, detection limit 12 ng/mL). pNbDR5$_4$ led to peak Nanobody plasma levels of 54 ± 27 ng/mL, which remained above 24 ± 5 ng/mL throughout the 12 weeks of follow-up (Figure 2A). pNbDR5-NbSA and pNbDR5$_4$-NbSA led to peak Nanobody plasma levels of 5.2 ± 1.5 and 7.8 ± 1.3 µg/mL, respectively (Figure 2B). As early as 10 days post gene transfer, in three out of five mice in the pNbDR5-NbSA group and in four out of five mice in the pNbDR5$_4$-NbSA group, Nanobody levels decreased below the detection limit (4 ng/mL). In the following weeks, however, Nanobody plasma levels gradually increased and reached values of 2.0 ± 0.6 µg/mL for pNbDR5-NbSA and 2.8 ± 1.1 µg/mL for pNbDR5$_4$-NbSA at week 12 (Figure 2B). The loss of Nanobody detection was most likely due to a transient anti-drug-antibody (ADA) response, targeted against the expressed Nanobody. The pNbDR5$_4$-NbSA format consequently resulted in 144-fold higher peak Nanobody plasma levels compared to those obtained with pNbDR5$_4$ at equimolar dosing. These data demonstrate prolonged *in vivo* Nanobody expression and extended Nanobody accumulation in circulation.

Efficacy of intramuscular DNA-based Nanobody gene transfer

We evaluated the therapeutic efficacy of intramuscular pNbDR5$_4$ and pNbDR5$_4$-NbSA delivery in a subcutaneous COLO 205 nude mice tumor model. An empty control plasmid (pNull, 2319 base pairs), identical except for the deletion of the Nanobody expression cassette, was included to mimic any impact of the plasmid. Mice received an equimolar dose of either 220 µg pNbDR5$_4$ (*n* = 9), 240 µg pNbDR5$_4$-NbSA (*n* = 9) or 80 µg pNull (*n* = 10)

equally spread across four muscles. An additional 120 μg dose group was included for pNbDR5$_4$-NbSA (n=10) to evaluate dose-related pharmacokinetics and efficacy.

All DNA-based Nanobody treatments resulted in prolonged Nanobody expression throughout follow-up. pNbDR5$_4$ led to peak levels of 271 ± 30 ng/mL, which remained above 109 ± 18 ng/mL during the 10 weeks of follow-up (Figure 3A). The 120 μg pNbDR5$_4$-NbSA dose gave peak Nanobody plasma levels of 19.6 ± 2.4 μg/mL, which remained above 10 μg/mL throughout eight weeks of follow-up. The 240 μg dose led to a proportional level of 38.3 ± 3.3 μg/mL, which remained above 20.0 ± 1.2 μg/mL throughout follow-up (Figure 3B), demonstrating dose-dependent Nanobody levels. The pNbDR5$_4$-NbSA format consequently resulted in 142-fold higher peak Nanobody plasma levels compared to those obtained with pNbDR5$_4$ at equimolar dosing.

Anti-tumor responses were observed for both DNA-based Nanobody formats. pNbDR5$_4$ gene transfer resulted in a significant difference in tumor volume compared to pNull starting from day seven ($P \leq 0.01$) and compared to pNbDR5$_4$-NbSA starting from day 14 ($P \leq 0.05$). Anti-tumor responses remained significant throughout follow-up until day 34 ($P \leq 0.001$-0.0001) (Figure 3C and Table S1). The durability of these anti-tumor responses was reflected by the significantly prolonged median survival of pNbDR5$_4$ over pNull and pNbDR5$_4$-NbSA ($P \leq 0.001$) (Figure 3D). pNbDR5$_4$-NbSA resulted in a significant difference in tumor volume compared to pNull on day eight for the high dose ($P \leq 0.05$) and day 10 for the low dose ($P \leq 0.05$). However, these anti-tumor responses were lost as soon as day 12 and remained borderline significant only for the high dose (Figure 3C and Table S1). Either pNbDR5$_4$-NbSA dose failed to prolong survival (Figure 3D), confirming an overall lower response compared to pNbDR5$_4$, despite comparable *in vitro* efficacy and the 142-fold higher Nanobody exposure (Figure 3A-B and Figure S1C). No complete responders were observed in any of the treatment groups during follow-up (Figure S2A).

To exclude that the presence of a 600 to 1000-fold excess of serum albumin *in vivo* might have compromised the functional properties of the $NbDR5_4$-NbSA, *in vitro* experiments were carried out in the presence of a comparable excess of serum albumin (up to 6000-fold, Figure S1D). These data indicate that albumin binding does not affect the intrinsic functional properties of $NbDR5_4$-NbSA.

Efficacy of intratumoral DNA-based Nanobody gene transfer

To gain more insight in the limited response observed after intramuscular $pNbDR5_4$-NbSA delivery, we evaluated the efficacy of intratumoral delivery in the COLO 205 tumor xenograft model. Equimolar doses of 220, 240 and 80 μg of $pNbDR5_4$ (n = 8), $pNbDR5_4$-NbSA (n = 8) and pNull (n = 8), respectively, were equally divided across four treatment days (day 6, 8, 10 and 13) (Figure 4A).

Nanobody levels in plasma were not detectable (< 4 ng/mL) after intratumoral delivery of $pNbDR5_4$ (data not shown). In the absence of systemic exposure, five out of eight mice demonstrated tumor regression in the first days following treatment. Two mice exhibited a complete response and remained tumor free until the end of follow-up, i.e. 30 weeks after tumor cell injection (Figure S2B). This corresponded to a significant difference in tumor volume starting from day 31 ($P \leq 0.05$), and a significantly prolonged median survival ($P \leq 0.05$) compared to pNull (Figure 4A-B). Intratumoral delivery of $pNbDR5_4$-NbSA resulted in a limited plasma exposure (50-600 ng/mL) in six out of eight mice (data not shown). Three out of eight mice demonstrated initial tumor regression after treatment (Figure S2B), but the overall response did not reach statistical significance compared to pNull during follow-up (Figure 4A-B).

Pharmacokinetics and efficacy of intramuscular DNA-based versus IV protein-based Nanobody delivery

To compare gene transfer with conventional Nanobody administration, intramuscular pDNA doses were compared with a 3 mg/kg IV protein injection. Assuming a mouse blood volume of 0.080 mL per gram of weight, the latter dose provides a theoretically maximal exposure of 37.5 µg/mL. This is in the same range as the peak levels observed after intramuscular delivery of 240 µg pNbDR5$_4$-NbSA (Figure 3B). Furthermore, a 3 mg/kg dose of a comparable tetravalent anti-DR5 Nanobody was previously found to induce potent anti-tumor responses in a COLO 205 tumor xenograft model [12]. D-PBS IV injections and pNull intramuscular gene transfer served as controls for the respective administration routes. To match to some extent the slow onset of Nanobody expression after gene transfer with the instant systemic exposure to IV protein treatment, the latter was delivered one day later than gene transfer.

In line with the previous intramuscular Nanobody gene transfer experiment, all DNA-based Nanobody treatments demonstrated prolonged Nanobody expression throughout follow-up. pNbDR5$_4$ gene transfer led to peak levels of 269 ± 31 ng/mL, which remained above 207 ± 33 ng/mL during the 10 weeks of follow-up (Figure 5A). pNbDR5$_4$-NbSA gene transfer resulted in peak Nanobody levels of 34.5 ± 2.5 µg/mL, which remained above 30.0 ± 3.1 µg/mL during the eight weeks of follow-up (Figure 5B). In this case, DNA-based delivery of the NbSA-fusion format resulted in 128-fold higher peak Nanobody plasma levels compared to those obtained with an equimolar dose of pNbDR5$_4$. Both DNA-based Nanobodies were still detectable in plasma of complete responders 40 weeks post intramuscular gene transfer. In line with expectations, protein treatments resulted in limited duration of Nanobody exposure. Detection of NbDR5$_4$ levels in plasma was nearly completely lost one day post treatment (Figure 5C). NbDR5$_4$-NbSA levels were detected in plasma up to seven days post treatment (Figure 5D).

In agreement with the previous intramuscular study, anti-tumor responses were observed for both DNA-based Nanobody formats. pNbDR5$_4$ gene transfer resulted in a significant difference in tumor volume compared to pNull ($P \leq 0.01$) by day nine, compared to NbDR5$_4$-NbSA by day 18 ($P \leq 0.05$), compared to NbDR5$_4$ by day 25 ($P \leq 0.05$) and compared to pNbDR5$_4$-NbSA by day 27 ($P \leq 0.05$). Anti-tumor responses remained significant throughout follow-up until day 27 ($P \leq 0.05$-0.0001) (Figure 5E and Table S2). The observed anti-tumoral responses were also reflected by the significantly prolonged median survival of pNbDR5$_4$ over all other groups ($P \leq 0.05$-0.01) (Figure 5F). One mouse in the pNbDR5$_4$ group demonstrated a complete response and remained tumor free until the end of follow-up, over 30 weeks after tumor cell injection (Figure S2C). The corresponding NbDR5$_4$ protein treatment resulted in a significant difference in tumor volume as soon as day nine compared to D-PBS ($P \leq 0.05$). However, the initial response was lost by day 12. The overall lower response of the NbDR5$_4$-NbSA protein treatment was reflected in the survival plot and the lack of complete responders (Figure 5B and Figure S2C). Compared to the previous intramuscular study, more profound anti-tumor responses were observed for pNbDR5$_4$-NbSA gene transfer resulting in a significant difference in tumor volume compared to pNull starting from day nine ($P \leq 0.05$). The anti-tumor response was maintained throughout follow-up compared to pNull ($P \leq 0.01$) (Figure 5E and Table S2). pNbDR5$_4$-NbSA did result in significantly prolonged median survival compared to NbDR5$_4$-NbSA ($P \leq 0.05$) and pNull ($P \leq 0.01$), respectively. In contrast, the corresponding NbDR5$_4$-NbSA protein treatment failed to show any response, despite extended exposure over NbDR5$_4$ protein treatment. Overall, both pNbDR5$_4$ and pNbDR5$_4$-NbSA treatments prolonged survival over their respective protein and control groups (Figure 5F).

DISCUSSION

In the current study, we combined our DNA-based delivery platform with various half-life engineered Nanobody formats to achieve prolonged expression and higher drug levels *in vivo*. Additionally, we assessed the therapeutic efficacy of this approach in a mouse tumor model.

Following intramuscular electrotransfer in BALB/c mice, the monovalent anti-DR5 Nanobody (15 kDa) was not detected. Likely, the *in vivo* expression was not sufficiently high to compensate for the fast clearance reported for monovalent Nanobodies [3]. To overcome the rapid clearance and improve the resulting drug levels in circulation, two half-life extension strategies were successfully implemented. A first strategy focused on valency increase. The designed tetravalent anti-DR5 Nanobody was roughly 60 kDa in size, just above the glomerular filtration threshold [19]. This shift from monovalent to tetravalent format resulted in detectable double digit ng/mL Nanobody plasma levels in BALB/c mice. In athymic nude mice, increasing the pDNA dose accordingly led to higher Nanobody plasma concentrations, which were detectable for at least 40 weeks post gene transfer. In contrast, the tetravalent Nanobody cleared within 24 hours when delivered IV as a protein. A second strategy focused on a NbSA-fusion design. DNA-based delivery of bivalent bispecific NbDR5-NbSA (30 kDa) and pentavalent bispecific $NbDR5_4$-NbSA (75 kDa) resulted in markedly improved levels over the tetravalent $NbDR5_4$, indicating that NbSA-fusion had a significant impact on Nanobody accumulation. Indeed, consistently throughout this study, the NbSA-fusion strategy increased the $NbDR5_4$-NbSA peak plasma levels by a factor 128 to 144 over $NbDR5_4$, reaching plasma concentrations as high as 40 µg/mL. Together, these pharmacokinetic data confirm our research hypotheses: intramuscular DNA-based gene transfer promotes prolonged Nanobody exposure over IV protein-based treatment, and an increase in the half-life of the *in vivo* expressed Nanobody leads to a proportional build-up in plasma concentration.

392 Expressed Nanobodies appeared to trigger a transient ADA response in BALB/c mice. ADAs
393 have previously been described for DNA-based antibodies from foreign species in immune
394 competent mice, typically 10-14 days after electroporation, often resulting in complete and
395 lasting loss of mAb detection [7]. In the current study, the presumed ADA response to the
396 expressed Nanobodies had only a limited impact on the pharmacokinetics, as illustrated by the
397 temporary drop in Nanobody detection. We previously observed ADA responses of such
398 transient nature following DNA-based mAb delivery in sheep [6].
399 In efficacy experiments, the low but continuous Nanobody exposure after intramuscular
400 pNbDR5$_4$ delivery induced a more potent and prolonged anti-tumor response than the rapidly
401 cleared IV NbDR5$_4$ protein injection. Comparably, pNbDR5$_4$-NbSA gene transfer improved
402 anti-tumor responses over the NbDR5$_4$-NbSA protein. Overall, DNA-based treatments
403 outperformed their respective protein treatments from both a pharmacokinetic and an efficacy
404 perspective.
405 Localized drug delivery, such as intratumoral administration, presents a rational approach
406 toward minimizing systemic exposure [20]. Indeed, the current study reports prolonged
407 systemic exposure after intramuscular pNbDR5$_4$ delivery and total absence of exposure after
408 intratumoral pNbDR5$_4$ delivery. However, intratumoral delivery increased the number of
409 complete responders over intramuscular delivery, indicating that DNA-based Nanobodies can
410 still prove effective in absence of systemic exposure. Despite differences in tumor model, our
411 exposure and efficacy findings are compatible with those observed after intratumoral delivery
412 of DNA-based mAbs [8]. This localized strategy may be interesting for drugs that exhibit
413 systemic toxicity, such as the tetravalent anti-DR5 Nanobody [15].
414 Throughout this study, anti-tumor responses were less potent for NbDR5$_4$-NbSA compared to
415 NbDR5$_4$, regardless of delivery form (protein or DNA) and route (muscle or tumor).
416 Considering NbDR5$_4$-NbSA and NbDR5$_4$ had similar *in vitro* activity irrespective of the

presence of albumin, the reduced efficacy of NbDR5$_4$-NbSA *in vivo* is unlikely caused by steric hindrance subsequent to binding to albumin. We therefore hypothesize that albumin binding either acts as a 'sink' for the drug in circulation or leads to rapid internalization in the tumor. In both cases, target binding and apoptotic signaling at the tumor site are compromised, resulting in a reduced *in vivo* efficacy. In contrast, a number of studies have proposed solid tumors as a site for albumin retention and have therefore pursued albumin binding as a tumor-targeting strategy [21]. In our model, however, albumin binding thus reduced *in vivo* efficacy.

To the best of our knowledge, intramuscular and intratumoral DNA-based Nanobody delivery have not been reported. Our preference for pDNA is based on the ease of engineering, large packaging capacity, straightforward production, and limited immunogenicity risks. Other delivery platforms, such as viral vectors and mRNA, have been used to express Nanobody formats. Overall, each have their specific benefits and challenges. Viral vectors generally drive stable and prolonged expression, but face limitations in terms of production, packaging capacity, and immunogenicity [22]. mRNA presents a quick onset but transient expression platform that typically requires repeated administration to obtain prolonged exposure [23], providing limited benefit over protein-based delivery. Moreover, dedicated formulations are required for mRNA administration and transfection, adding to the CMC (Chemistry, Manufacturing and Controls) challenge.

By means of adenoviral vectors, peak Nanobody levels above one mg/mL have been achieved in mice, which vary greatly from 0.01 ng/ml to >100 µg/ml six to eight weeks post-treatment [24,25]. In one study, a bivalent Nanobody binding Botulinum toxin A and fused to an albumin-binding peptide, was detected in the serum of two mice at least 18 weeks post treatment between levels of 0.1 – 1 µg/mL. mRNA-based expression of the same Nanobody resulted in peak serum levels of 300 µg/mL 24 h after administration. These levels, however,

quickly dropped below 50 µg/mL after five days, after which Nanobody titers were not reported [26]. Not taking into consideration the differences in study design, the peak Nanobody plasma levels in the current study are roughly 5- to 25-fold lower than for mRNA-based and viral-vector-mediated delivery, respectively. The higher expression titers with viral vectors and mRNA are linked to a more efficient transfection. This, however, also implies a higher risk of transfecting undesirable tissues. For pDNA, this is less of a concern, since transfection is enabled by electroporation, a clinical delivery approach that allows for a highly controlled and safe tissue transfection, i.e. within the applied electrical field [5]. In terms of expression duration, we found Nanobody in plasma for at least 40 weeks after delivery of the encoding DNA, which is the longest follow-up reported for this approach, irrespective of expression platform.

Next to the reported findings, DNA-encoded Nanobodies can have some specific advantages. The modular nature of Nanobodies and the large capacity of plasmid backbones make a perfect fit for combination strategies expressing multiple and/or complex multispecific Nanobodies *in vivo*. Furthermore, DNA-based delivery can be used as a tool for pre-clinical *in vivo* lead selection, without the need for *in vitro* protein production and purification steps.

In conclusion, the current study provides pre-clinical proof of concept for DNA-based Nanobody gene transfer. Intramuscular delivery of DNA-based half-life engineered Nanobodies led to prolonged and substantially higher Nanobody plasma exposure. Furthermore, Nanobody gene transfer showed improved therapeutic efficacy over conventional protein delivery. Overall, the reported data highlight the potential of DNA-based Nanobodies in oncology and broaden the application range of DNA-based therapeutics.

ACKNOWLEDGMENTS

The authors wish to thank Ablynx for providing access to the Nanobody sequences as well as the Nanobody-binding monoclonal antibodies, and Carlo Boutton (Ablynx) and Pieter Deschaght (Ablynx) for their useful suggestions. The authors also express thanks to Liesl Jacobs for her valuable input on intratumoral gene transfer.

CONFLICTS OF INTEREST

KH received consulting fees from OncoSec Medical (San Diego, CA, USA). All other authors declare no competing interests.

FUNDING

This research is supported by Research Foundation - Flanders (FWO: PhD mandate 1S50617N to G.V.; research project G0E2117N to P.D. and K.H.), KU Leuven (C2 grant: C22/15/024 to P.D. and K.H.), and Flanders Innovation & Entrepreneurship (VLAIO: IWT.150743 to K.H.).

REFERENCES

1. Muyldermans S. Nanobodies: natural single-domain antibodies. Annu Rev Biochem. 2013;82:775-97.

2. Jovčevska I, Muyldermans S. The Therapeutic Potential of Nanobodies. BioDrugs. 2019.

3. Hoefman S, Ottevaere I, Baumeister J, Sargentini-Maier M. Pre-Clinical Intravenous Serum Pharmacokinetics of Albumin Binding and Non-Half-Life Extended Nanobodies®. Antibodies. 2015;4(3):141-56.

4. Hollevoet K, Declerck PJ. State of play and clinical prospects of antibody gene transfer. J Transl Med. 2017;15(1):131.

5. Heller R, Heller LC. Gene electrotransfer clinical trials. Adv Genet. 2015;89:235-62.

6. Hollevoet K, De Vleeschauwer S, De Smidt E, Vermeire G, Geukens N, Declerck P. Bridging the Clinical Gap for DNA-based Antibody Therapy through Translational Studies in Sheep. Hum Gene Ther. 2019.

7. Hollevoet K, De Smidt E, Geukens N, Declerck P. Prolonged in vivo expression and anti-tumor response of DNA-based anti-HER2 antibodies. Oncotarget. 2018;9(17):13623-36.

8. Jacobs L, De Smidt E, Geukens N, Declerck P, Hollevoet K. DNA-based delivery of checkpoint inhibitors in muscle and tumor enables long-term responses with distinct exposure. Molecular Therapy. 2020.

9. Duperret EK, Trautz A, Stoltz R, Patel A, Wise MC, Perales-Puchalt A, et al. Synthetic DNA-Encoded Monoclonal Antibody Delivery of Anti-CTLA-4 Antibodies Induces Tumor Shrinkage In Vivo. Cancer Res. 2018;78(22):6363-70.

10. Pan H, Liu J, Deng W, Xing J, Li Q, Wang Z. Site-specific PEGylation of an anti-CEA/CD3 bispecific antibody improves its antitumor efficacy. Int J Nanomedicine. 2018;13:3189-201.

11. Iqbal U, Trojahn U, Albaghdadi H, Zhang J, O'Connor-McCourt M, Stanimirovic D, et al. Kinetic analysis of novel mono- and multivalent VHH-fragments and their application for molecular imaging of brain tumours. Br J Pharmacol. 2010;160(4):1016-28.

12. Huet HA, Growney JD, Johnson JA, Li J, Bilic S, Ostrom L, et al. Multivalent nanobodies targeting death receptor 5 elicit superior tumor cell killing through efficient caspase induction. MAbs. 2014;6(6):1560-70.

13. Dong HP, Kleinberg L, Silins I, Florenes VA, Trope CG, Risberg B, et al. Death receptor expression is associated with poor response to chemotherapy and shorter survival in metastatic ovarian carcinoma. Cancer. 2008;112(1):84-93.

14. Wiezorek J, Holland P, Graves J. Death receptor agonists as a targeted therapy for cancer. Clin Cancer Res. 2010;16(6):1701-8.

15. Papadopoulos KP, Isaacs R, Bilic S, Kentsch K, Huet HA, Hofmann M, et al. Unexpected hepatotoxicity in a phase I study of TAS266, a novel tetravalent agonistic Nanobody(R) targeting the DR5 receptor. Cancer Chemother Pharmacol. 2015;75(5):887-95.

16. Cromie K, Dombrecht B, Ettenberg S, Kolkman J, Li J, Meerschaert K, et al., inventors; Ablynx N.V. (Zwijnaarde, BE), Novartis A.G. (Basel, CH), assignee. Agonist Dr5 Binding Polypeptides patent WO 2011/098520 A1. 2011/02/10.

17. Staelens S, Steffensen S, Morizzo E, Ponsaert RAF, Ottevaere I, Cerdobbel AN, inventors; ABLYNX NV, assignee. Improved Serum Albumin Binding Immunoglobulin Single Variable Domains patent WO 2018/104444 A1. 2017/12/07.

18. Lee S-C, Cheong H-J, Kim S-J, Yoon J, Kim HJ, Kim KH, et al. Low-Dose Combinations of LBH589 and TRAIL Can Overcome TRAIL-resistance in Colon Cancer Cell Lines. Anticancer Research. 2011;31(10):3385-94.

19. Briggs JP, Kriz W, Schnermann JB. Overview of Kidney Function and Structure. In: Gilbert SJ, Weiner DE, editors. National Kidney Foundation Primer on Kidney Diseases2014. p. 2-18.

20. Fumoto S, Kawakami S, Hashida M, Nishida K. Targeted Gene Delivery: Importance of Administration Routes. In: Wei M, Good D, editors. Novel Gene Therapy Approaches2013. p. 3-31.

21. Hoogenboezem EN, Duvall CL. Harnessing albumin as a carrier for cancer therapies. Adv Drug Deliv Rev. 2018;130:73-89.

22. Mali S. Delivery systems for gene therapy. Indian J Hum Genet. 2013;19(1):3-8.

23. Pardi N, Secreto AJ, Shan X, Debonera F, Glover J, Yi Y, et al. Administration of nucleoside-modified mRNA encoding broadly neutralizing antibody protects humanized mice from HIV-1 challenge. Nat Commun. 2017;8:14630.

24. Moayeri M, Tremblay JM, Debatis M, Dmitriev IP, Kashentseva EA, Yeh AJ, et al. Adenoviral Expression of a Bispecific VHH-Based Neutralizing Agent That Targets Protective Antigen Provides Prophylactic Protection from Anthrax in Mice. Clin Vaccine Immunol. 2016;23(3):213-8.

25. Mukherjee J, Dmitriev I, Debatis M, Tremblay JM, Beamer G, Kashentseva EA, et al. Prolonged prophylactic protection from botulism with a single adenovirus treatment promoting serum expression of a VHH-based antitoxin protein. PLoS One. 2014;9(8):e106422.

26. Thran M, Mukherjee J, Ponisch M, Fiedler K, Thess A, Mui BL, et al. mRNA mediates passive vaccination against infectious agents, toxins, and tumors. EMBO Mol Med. 2017;9(10):1434-47.

FIGURE LEGENDS

Figure 1 | Overview of evaluated DNA-based Nanobody formats

This figure depicts the four different anti-DR5 Nanobody formats cloned into an optimized plasmid for expression *in vivo*. Bispecific Nanobodies bind to both DR5 and SA. PK, pharmacokinetics; DR5, human death receptor 5; SA, serum albumin; αDR5, human anti-death-receptor 5 Nanobody unit; αSA, human/mouse anti-serum albumin Nanobody unit.

Figure 2 | Nanobody plasma levels after intramuscular gene transfer in BALB/c mice

Nanobody plasma levels over weeks post intramuscular (IM) electroporation (EP) for (A) monospecific pNbDR5 and pNbDR5$_4$ gene transfer groups and (B) bispecific pNbDR5-NbSA and pNbDR5$_4$-NbSA gene transfer groups.

Figure 3 | Tumor growth, survival and Nanobody plasma levels after intramuscular DNA-based Nanobody gene transfer in nude mice

Nanobody plasma levels over weeks post intramuscular (IM) electroporation (EP) for (A) pNbDR5$_4$ and (B) pNbDR5$_4$-NbSA. (C) Tumor volume over days post subcutaneous (SC) tumor cell injection shown for the intramuscular gene transfer treatment cohorts. Start of DNA-based treatment marked by arrow. Significant differences in tumor volume are detailed in Table S1. (D) Survival curves of the respective cohorts. *** $P \leq 0.001$

Figure 4 | Tumor growth and survival plot after intratumoral DNA-based gene transfer in nude mice

(A) Tumor volume over days post subcutaneous (SC) tumor cell injection shown for intratumoral gene transfer treatment cohorts. Total DNA dose was divided equally over four treatment days at day 6, 8, 10 and 13, marked by arrows. Significant differences in tumor

volume compared to pNbDR5$_4$ are indicated at individual time points. (B) Survival curves of the respective cohorts. * $P \leq 0.05$

Figure 5 | Nanobody plasma levels, tumor growth and survival plots after intramuscular DNA-based gene transfer or intravenous Nanobody infusion in nude mice

Nanobody plasma levels over time post treatment for (A) intramuscular (IM) electroporation (EP) of pNbDR5$_4$, (B) IM EP of pNbDR5$_4$-NbSA, (C) intravenous (IV) injection of NbDR5$_4$ and (D) IV injection of NbDR5$_4$-NbSA. For IV treatments, the first sample was taken after 1hr. (E) Tumor volume over days post subcutaneous (SC) tumor cell injection shown for IM DNA-based, IV protein-based and control cohorts. DNA-based delivery marked by arrow at day six. IV protein dosing marked by arrow at day seven. Significant differences in tumor volume are detailed in Table S2. (F) Survival curves of the respective cohorts. Significance levels compared to pNbDR5$_4$ and pNbDR5$_4$-NbSA are indicated for the respective treatment groups. * $P \leq 0.05$; ** $P \leq 0.01$

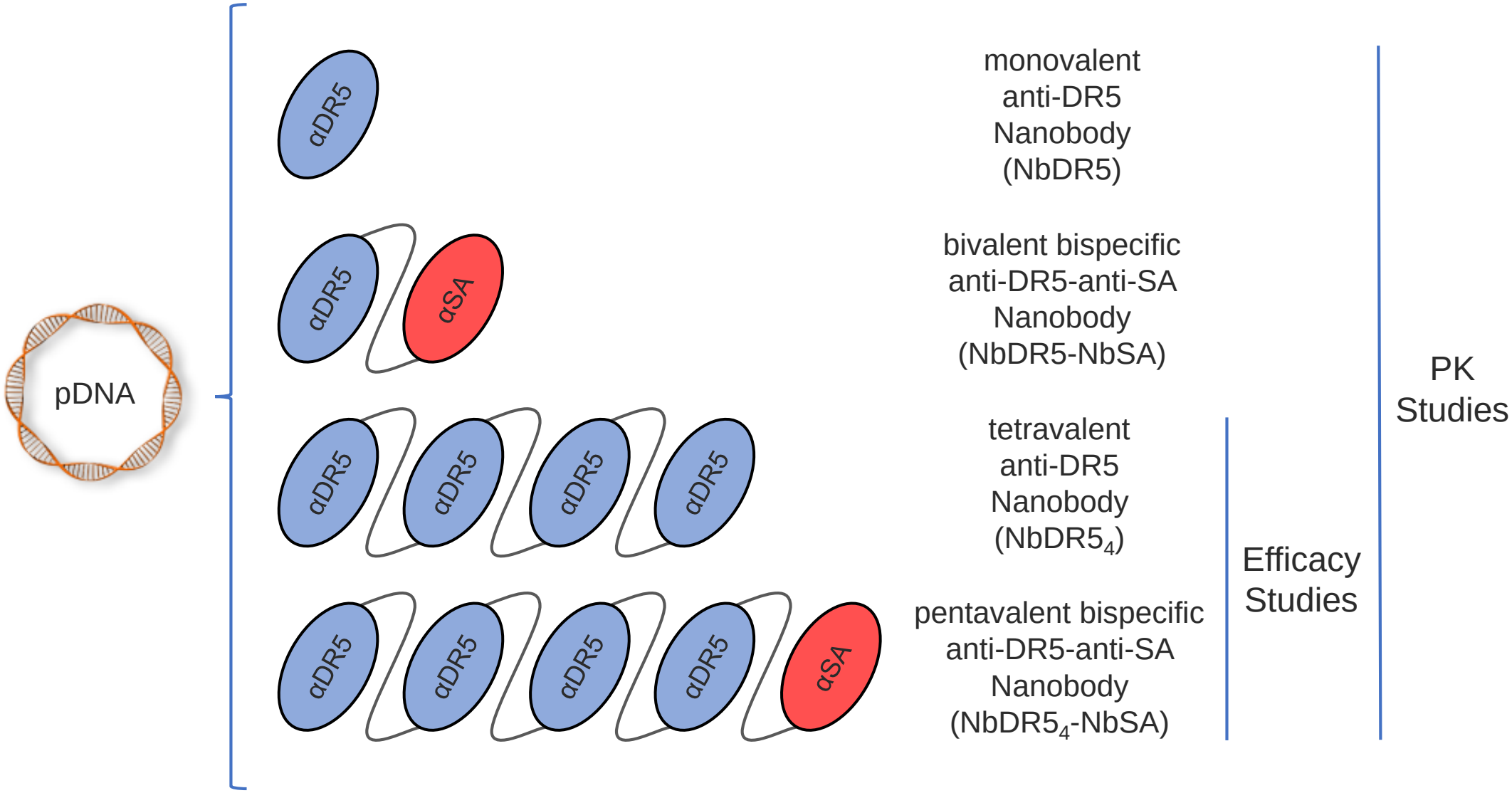
pDNA
αDR5
αDR5
αSA
αDR5
αDR5
αDR5
αDR5
αDR5
αDR5
αDR5
αDR5
αSA
monovalent anti-DR5 Nanobody (NbDR5)
bivalent bispecific anti-DR5-anti-SA Nanobody (NbDR5-NbSA)
tetravalent anti-DR5 Nanobody (NbDR5$_4$)
pentavalent bispecific anti-DR5-anti-SA Nanobody (NbDR5$_4$-NbSA)
Efficacy Studies
PK Studies

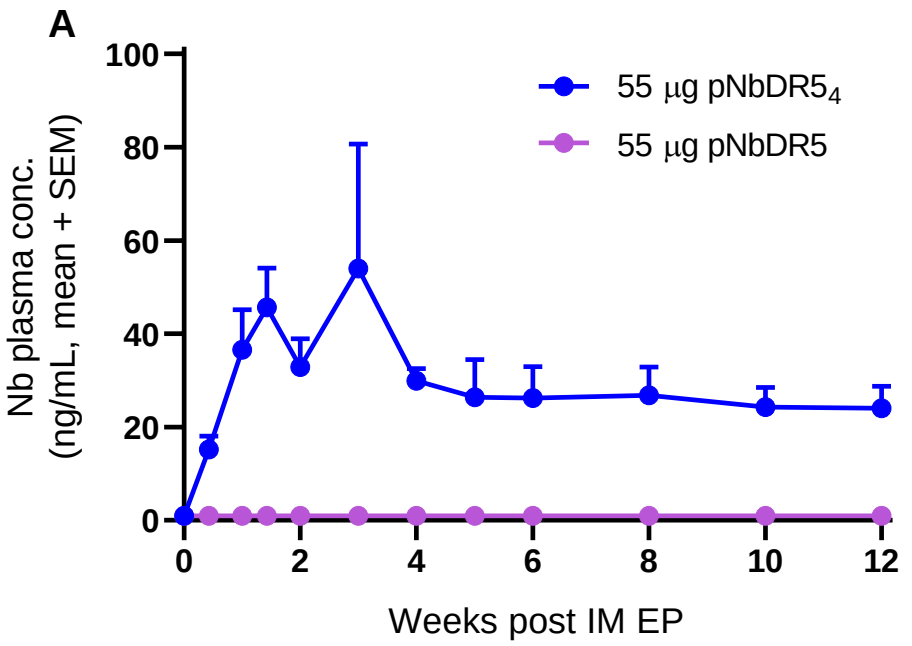
A
100
80
60
40
20
0
Nb plasma conc.
(ng/mL, mean + SEM)
55 μg pNbDR5$_4$
55 μg pNbDR5
0
2
4
6
8
10
12
Weeks post IM EP

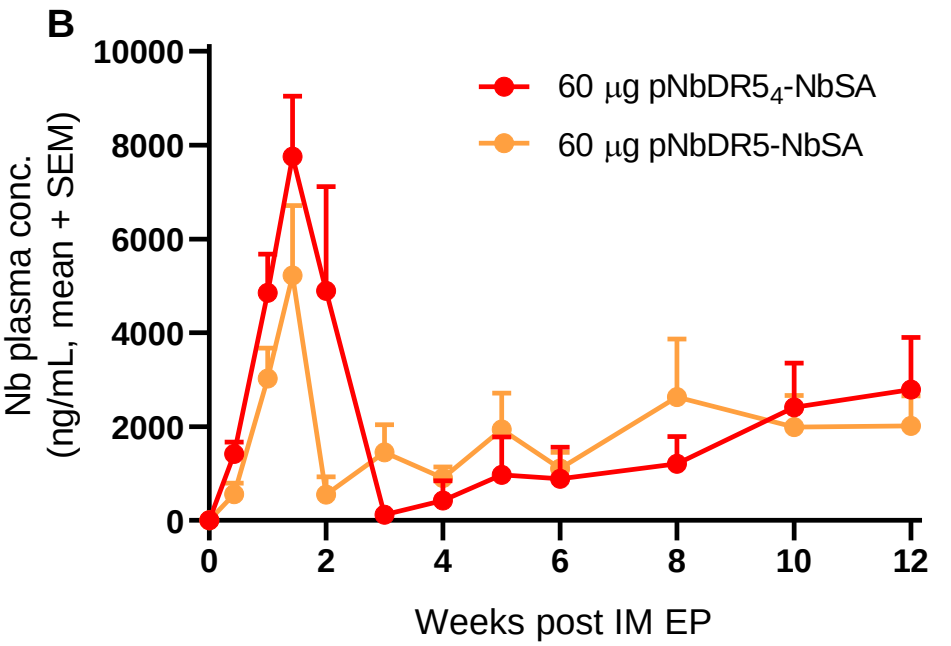
B
10000
8000
6000
4000
2000
0
Nb plasma conc.
(ng/mL, mean + SEM)
60 μg pNbDR5$_4$-NbSA
60 μg pNbDR5-NbSA
0
2
4
6
8
10
12
Weeks post IM EP

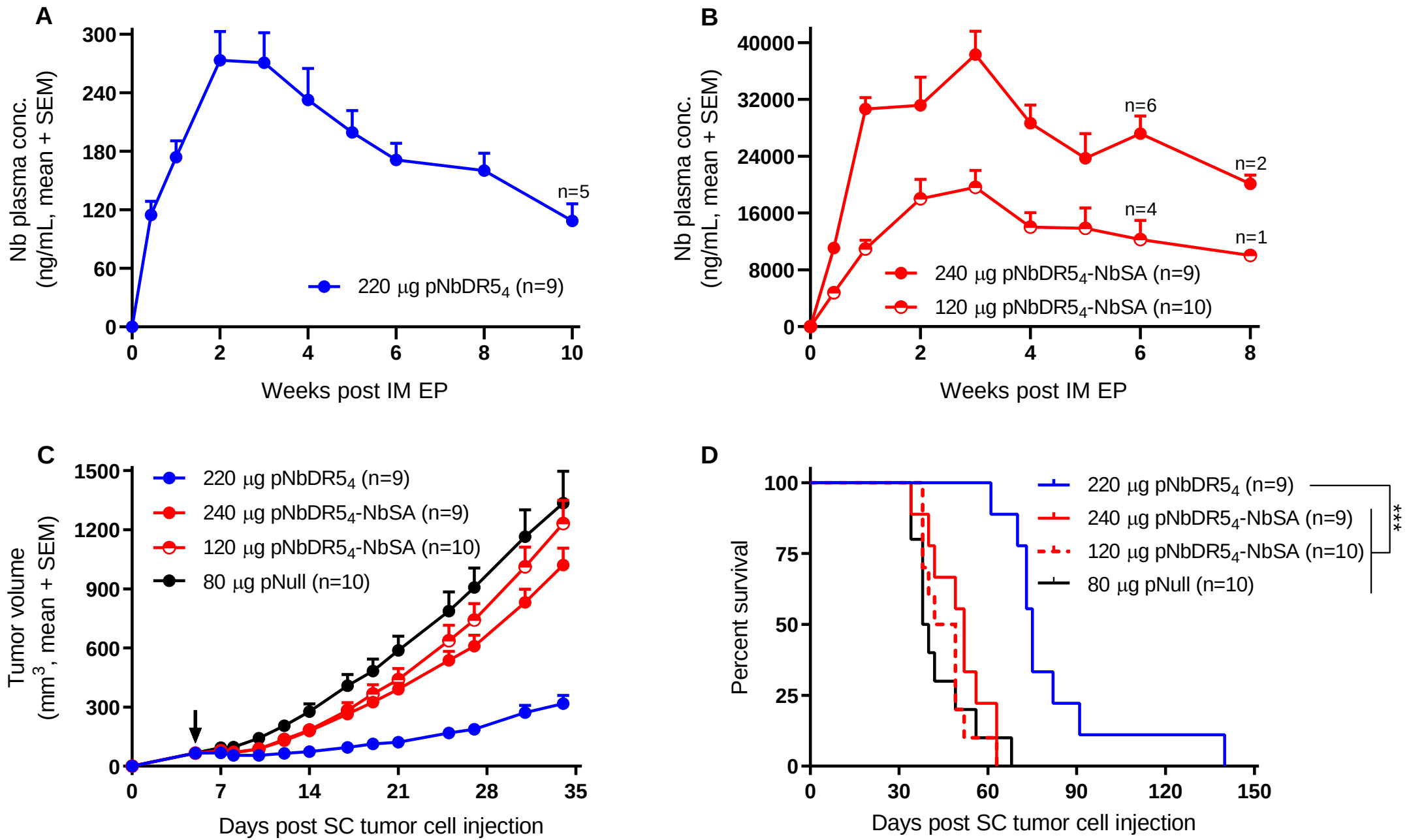
A
Nb plasma conc.
(ng/mL, mean + SEM)
300
240
180
120
60
0
0
2
4
6
8
10
Weeks post IM EP
n=5
220 μg pNbDR5$_4$ (n=9)
B
Nb plasma conc.
(ng/mL, mean + SEM)
40000
32000
24000
16000
8000
0
0
2
4
6
8
Weeks post IM EP
n=6
n=2
n=4
n=1
240 μg pNbDR5$_4$-NbSA (n=9)
120 μg pNbDR5$_4$-NbSA (n=10)
C
Tumor volume
(mm^3, mean + SEM)
1500
1200
900
600
300
0
0
7
14
21
28
35
Days post SC tumor cell injection
220 μg pNbDR5$_4$ (n=9)
240 μg pNbDR5$_4$-NbSA (n=9)
120 μg pNbDR5$_4$-NbSA (n=10)
80 μg pNull (n=10)
D
Percent survival
100
75
50
25
0
0
30
60
90
120
150
Days post SC tumor cell injection
220 μg pNbDR5$_4$ (n=9)
240 μg pNbDR5$_4$-NbSA (n=9)
120 μg pNbDR5$_4$-NbSA (n=10)
80 μg pNull (n=10)
****

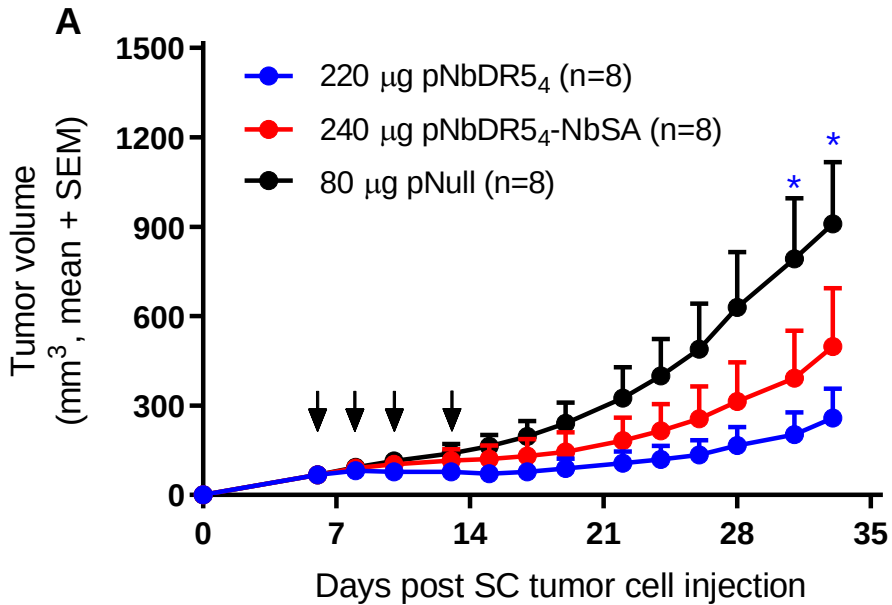
A
1500
1200
900
600
300
0
Tumor volume
(mm3, mean + SEM)
220 μg pNbDR54 (n=8)
240 μg pNbDR54-NbSA (n=8)
80 μg pNull (n=8)
*
*
0
7
14
21
28
35
Days post SC tumor cell injection

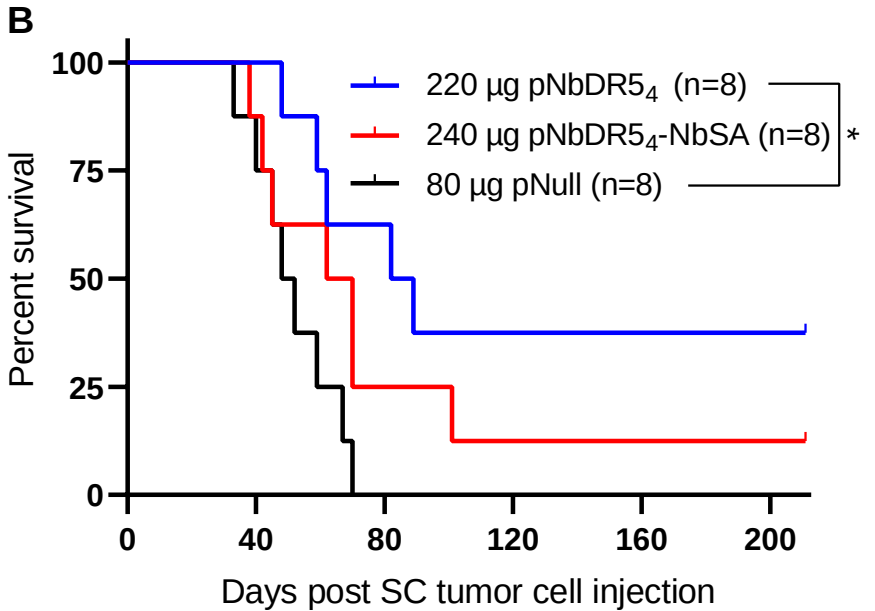
B
100
75
50
25
0
Percent survival
220 μg pNbDR54 (n=8)
240 μg pNbDR54-NbSA (n=8)
80 μg pNull (n=8)
*
0
40
80
120
160
200
Days post SC tumor cell injection

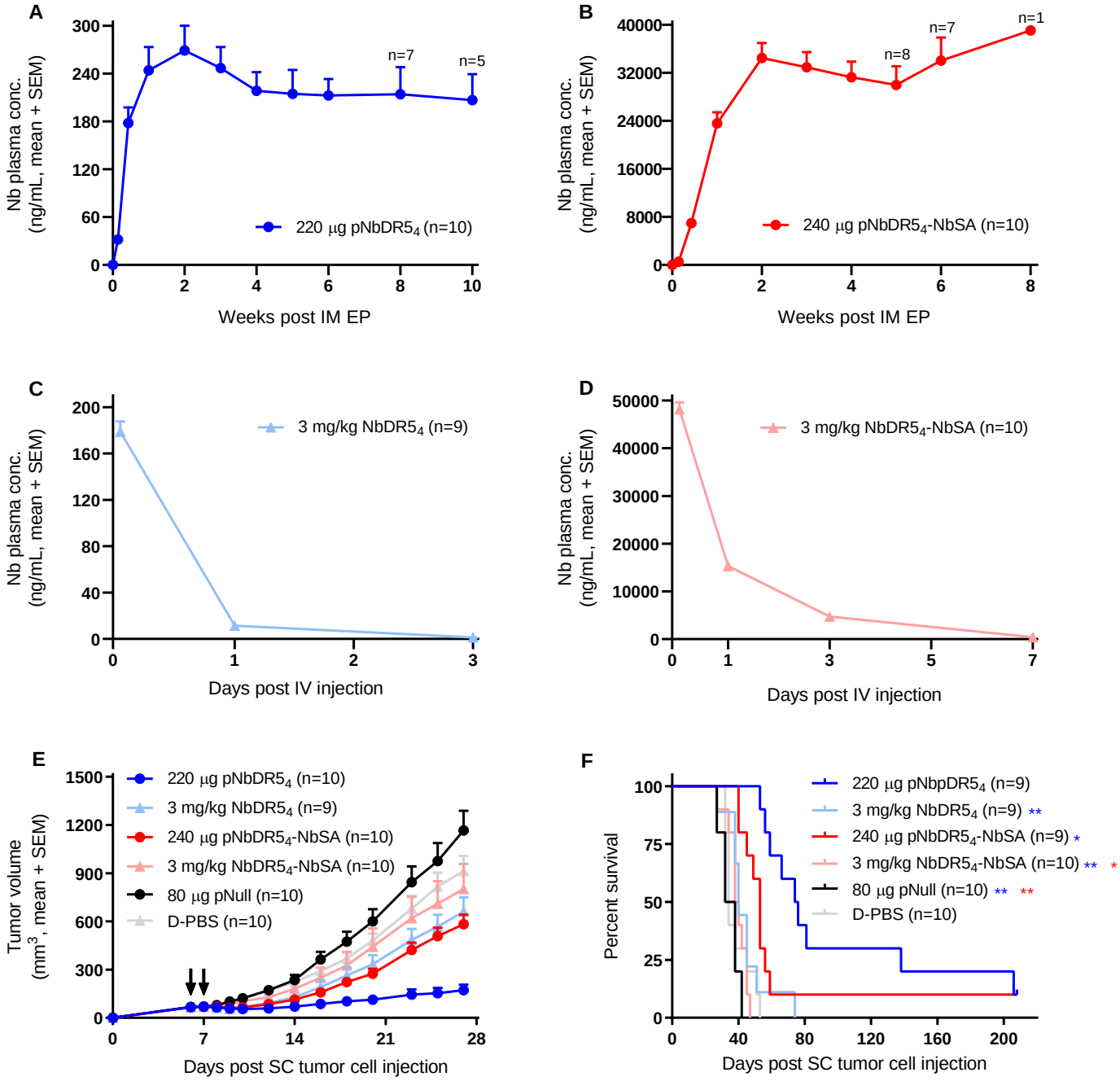
A
Nb plasma conc. (ng/mL, mean + SEM)
300
240
180
120
60
0
n=7
n=5
220 µg pNbDR5$_4$ (n=10)
0
2
4
6
8
10
Weeks post IM EP
B
Nb plasma conc. (ng/mL, mean + SEM)
40000
32000
24000
16000
8000
0
n=8
n=7
n=1
240 µg pNbDR5$_4$-NbSA (n=10)
0
2
4
6
8
Weeks post IM EP
C
Nb plasma conc. (ng/mL, mean + SEM)
200
160
120
80
40
0
3 mg/kg NbDR5$_4$ (n=9)
0
1
2
3
Days post IV injection
D
Nb plasma conc. (ng/mL, mean + SEM)
50000
40000
30000
20000
10000
0
3 mg/kg NbDR5$_4$-NbSA (n=10)
0
1
3
5
7
Days post IV injection
E
Tumor volume (mm^3, mean + SEM)
1500
1200
900
600
300
0
220 µg pNbDR5$_4$ (n=10)
3 mg/kg NbDR5$_4$ (n=9)
240 µg pNbDR5$_4$-NbSA (n=10)
3 mg/kg NbDR5$_4$-NbSA (n=10)
80 µg pNull (n=10)
D-PBS (n=10)
0
7
14
21
28
Days post SC tumor cell injection
F
Percent survival
100
75
50
25
0
220 µg pNbpDR5$_4$ (n=9)
3 mg/kg NbDR5$_4$ (n=9) **
240 µg pNbDR5$_4$-NbSA (n=9) *
3 mg/kg NbDR5$_4$-NbSA (n=10) ** *
80 µg pNull (n=10) ** **
D-PBS (n=10)
0
40
80
120
160
200
Days post SC tumor cell injection